β decay studies of $^{109,107}Sb$

J. J. Ressler,[1,2,3] W. B. Walters,[1] D. S. Brenner,[4] C. N. Davids,[2] A. Heinz,[2] G.-L. Poli,[2] J. Shergur,[1] and D. Seweryniak[2]
[1]*Department of Chemistry, University of Maryland, College Park, Maryland 20742*
[2]*Physics Division, Argonne National Laboratory, Argonne, Illinois 60439*
[3]*A. W. Wright Nuclear Structure Laboratory, Yale University, New Haven, Connecticut 06520*
[4]*Department of Chemistry, Clark University, Worcester, Massachusetts 01610*
(Received 21 December 2001; published 5 April 2002)

Low-spin, low energy-levels in $^{109,107}Sn$ have been studied following the β-decay of a 17-s ^{109}Sb and a 4-s ^{107}Sb, respectively. A number of new transitions and levels are established in ^{109}Sn with improved support for spin and parity assignments for previously known states. In addition, the presence of two pairs of levels separated by only 14 keV is confirmed. Four new levels are observed in ^{107}Sn, three of them are below 1 MeV excitation energy. The structure of these nuclides is discussed, focusing on three-quasiparticle cluster structures, movement of the Fermi level, and extrapolations for the single-neutron levels in ^{101}Sn.

DOI: 10.1103/PhysRevC.65.044330 PACS number(s): 23.40.−s, 23.20.Lv

I. INTRODUCTION

Excitation energies for the single-neutron $d_{5/2}, g_{7/2}, d_{3/2}$, $s_{1/2}$, and $h_{11/2}$ levels in the closed proton shell nuclei ^{79}Ni, ^{91}Zr, ^{101}Sn, and ^{131}Sn are the foundation for mapping monopole shifts of neutron levels in the $N=50$ shell to $N=82$ shell. These shifts serve as the basis for shell model calculations and other theoretical work in this mass region [1]. In addition, the $d_{5/2}$-$s_{1/2}$ and $g_{7/2}$-$d_{3/2}$ separation energies are important for calculations of $E2$ transition rates for valence neutrons.

Unfortunately, no data are presently available for ^{79}Ni or ^{101}Sn. Estimates for the single-neutron levels are therefore inferred from observations in the neighboring nuclei. A general lack of data in the light Sn isotopes may cause erroneous assumptions for the neutron single-particle levels near $A=100$. In this paper, new data for energies, spins, and parities of levels in $^{109,107}Sn$ have been sought following β decay of $^{109,107}Sb$. β-decay experiments were chosen as the low-spin states would be favorably populated. For both isotopes, the parent Sb is comprised of a $\pi d_{5/2} 5/2^+$ ground state that will preferentially populate $\nu d_{3/2}\,3/2^+$ levels in the daughter via Gamow-Teller spin-flip β-decay transitions. A significant intensity will also feed many other low-spin states with suitable wave function overlaps with the parent. This new information is complementary to high-spin structure data available for odd-$A^{105-111}Sn$ and the recently observed excited states of ^{103}Sn [2,3]. These data may also be compared with numerous theoretical calculations available in the literature.

II. EXPERIMENTS

The 17-s ^{109}Sb nuclei were produced using a 230-MeV ^{58}Ni beam from the ATLAS heavy-ion accelerator at Argonne National Laboratory on a 477-μg/cm^2 ^{54}Fe target. Recoiling reaction products were separated by mass/charge ratios through the Argonne fragment mass analyzer (FMA) and implanted onto the tape of a moving tape collector (MTC). The FMA was tuned to select recoils of $A=109$ with $Q=25$; nuclei with $A=108$ and $Q=25$ are produced with a higher cross section and form a tail under the $A=109$ recoil peak exiting the FMA. Mechanical slits were used on either side of the FMA focal plane to reduce the intensity of the $A=108$ recoils.

The MTC tape was advanced at 30 s intervals to a shielded counting station comprised of two large-volume (80% and 120%) HPGe detectors placed as close as possible to the tape. An additional 80% HPGe detector was hung from above at a distance of ~10 cm from the tape. Aluminum β absorbers of 1 cm thickness were placed in front of each detector. γ-singles, γ-γ coincidences, and γ-time data were collected and analyzed.

The setup was slightly modified for the production and decay of ^{107}Sb. A 260-MeV ^{58}Ni beam was used with a 635-μg/cm^2 ^{54}Fe target to produce the 4-s ^{107}Sb in the $3p2n$ fusion-evaporation channel. The $A=107$ reaction products were mass/charge separated through the FMA and implanted onto the tape of an MTC. The FMA was set to select recoils of $A=107$ and $Q=25$. As before, mechanical slits were used at the focal plane to minimize the intensity of the strongly produced $A=106$ recoils.

The MTC tape was advanced at 9 s intervals to a shielded detector station. A 1-cm-thick detector for low-energy γ rays [low-energy photon spectrometer] (LEPS) was placed across a 70% HPGe detector as close as possible to the tape transport pipe. As in the $A=109$ experiment, an 80% HPGe was hung from above at a distance of ~10 cm from the tape. Aluminum β absorbers were placed in front of the 70% and 80% HpGe's but not the LEPS. γ-singles, γ-γ coincidences, and γ-time data were collected and analyzed.

III. RESULTS

β-decay studies of ^{109}Sb and ^{107}Sb were presented initially by Johnston *et al.* [4] and Shibata *et al.* [5], respectively. Their results were subsequently confirmed and augmented in a relatively low-statistics study [6]. The data presented in this paper further confirms previous observations with significantly improved statistics. In addition, new levels in ^{109}Sn and ^{107}Sn are identified.

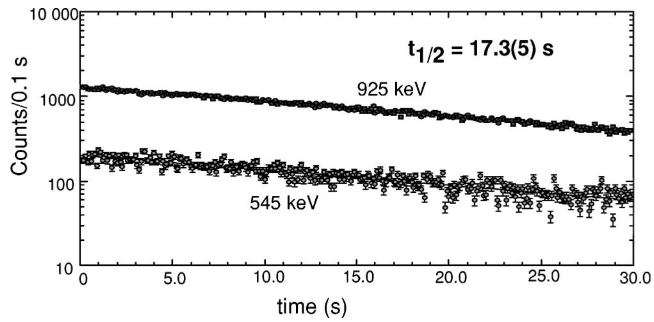

FIG. 1. Half-life determination for ^{109}Sb. Intensities of the 925- and 545-keV transitions are shown as a function of time following a tape movement. A weighted least-squares fit to these data gives 17.3(5) s for the β^+/EC-decay half-life of ^{109}Sb.

A. ^{109}Sn

The half-life for the ^{109}Sb β^+/EC decay has been determined to a slightly higher precision. Intensities of the 925 and 545 keV transitions are shown in Fig. 1 as a function of time relative to the last tape move. A 17.3(5) s half-life was determined by a least-squares fit to these data. Our value is in good agreement with the half-life of 17.0(7) s reported by Johnston *et al.* [4].

Transition energies and intensities for ^{109}Sn were deduced from γ-singles, γ-γ coincidences, and γ-time data. γ transitions from $A=109$ isobars and strongly produced $A=108$ nuclei are observed in the singles spectrum. An example of the singles spectrum is shown in Fig. 2(a). Some γ transition intensities could not be derived directly from the singles data due to energy overlaps with neighboring nuclei. In a two-dimensional plot of γ energy versus time, projections of γ-ray energies for specific times were used to help determine correct intensities.

A spectrum of transitions belonging only to short-lived species was created by subtracting all events detected between 15.0 and 29.8 s from events detected within 14.8 s following a tape move. Short-lived species decay away during the early period, and are manifested as peaks in the subtracted spectrum. Long-lived species decay equally during both the collection times and subtract approximately to zero. In this manner, contamination from background and long-lived transitions having an equal, or nearly equal, energy transition as assigned to ^{109}Sn could be removed and the ^{109}Sn transition intensity measured accurately. An example is shown in Figs. 2(b–d).

A similar spectrum showing only long-lived species could also be created to remove contamination from very short-lived species. Events detected within 6.5 s following a tape move were subtracted from the events detected between 7.5 and 29.8 s. The 7.6-s^{108}Sb and 4.6-s^{109}Te transitions subtract to zero while the longer-lived species produce peaks in the resultant spectrum.

Intensities for a few weak transitions and ^{109}Sn doublets could not be determined from γ-singles or time subtraction data. For these transitions, coincidence data were used to determine the proper intensity. Peaks were fit as above, and weak intensities scaled relative to a known γ transition also present in the coincidence spectrum. Due to the lower statistics observed in the coincidence spectra, uncertainties for the peak areas are slightly larger.

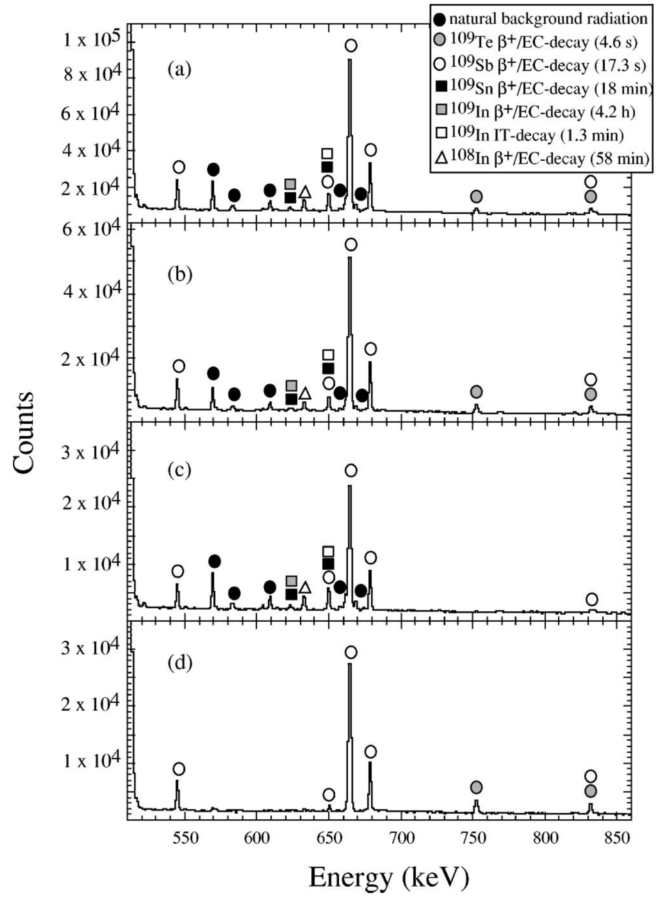

FIG. 2. Singles and time-gated γ-energy spectra for $A=109$. Figure 2(a) shows the singles spectrum for all $A=109$ recoils independent of time. Figure 2(b) displays all the transitions detected within approximately 15 s following a tape move. Figure 2(c) shows transitions detected later than 15 s following a tape move. Figure 2(d) shows the subtraction of the late time spectrum from the earlier time. Long-lived components subtract to zero, while short-lived transitions appear as peaks.

The intensity for the 1064-keV decay from the 1078-keV level was adopted from Dankó *et al.* [7]. Energy coincidences for the 835- and 932-keV γ's feeding the 1078-keV level suggested a very low 1064-keV decay intensity relative to the 1078-keV transition intensity. However, coincidences with the 571-keV γ suggested a very strong branch to the 14-keV level relative to the ground. Due to the lack of consistency, a 22% branch to the 14-keV level suggested by Ref. [7] was used.

In Table I, all transition intensities are shown relative to the 925-keV transition. Peak energies, areas, and errors were determined by fitting Gaussian shapes to the peaks using the RADWARE software package [8]. For intensities determined by coincidences, peaks were fit as above and scaled relative to a known γ intensity also present in the coincident spectrum. The proposed β-decay scheme for ^{109}Sb$\rightarrow$^{109}Sn is shown in Figs. 3 and 4.

Transitions were placed in the energy level scheme primarily by the coincidence data. The time data were useful in the

TABLE I. γ intensities in ^{109}Sn following ^{109}Sb β decay. Energy errors are ± 0.3 keV. Intensities are relative to the 925 keV transition.

Level energy (keV)	To level (keV)	γ-ray energy (keV)	Relative intensity
0			
14			
545	0	544.4	11.2(1)
664	14	650.1	1.3(1)
	0	664.0	39(2)
678	14	664.2	24(2)
	0	678.3	20.2(2)
925	678	246.6	2.8(1)
	664	260.8	6.4(2)
	545	381.3	0.6(2)
	14	910.9	2.9(2)
	0	925.0	100
991	545	446.3	0.4(1)
	0	991.2	1.8(1)
1062	664	397.5	3.0(7)
	545	516.5	4(1)
	14	1047.7	4.8(1)
	0	1061.8	67.9(7)
1078	14	1064	0.8(2)
	0	1078	3.8(1)
1229	678	550.2	0.6(1)
	14	1214.4	1.1(1)
	0	1229.3	7.7(1)
1343	678	665.8	0.5(1)
	0	1343.7	2.3(1)
1496	1078	433.6	0.5(1)
	664	831.4	2.1(6)
	545	951.1	2.4(2)
	14	1482.2	1.7(1)
	0	1496.1	28.3(2)
1614	925	687.3	0.4(1)
	678	936.2	3.2(2)
	14	1601.4	3.8(2)
1649	1078	571.3	0.8(1)
	664	985.5	1.1(2)
	545	1104.4	2.7(2)
	14	1636.3	1.6(2)
	0	1650.4	3.1(2)
1914	1229	685	$\leqslant 1.0$
	1078	835.0	0.6(2)
	664	1249.4	1.8(5)
	545	1369.6	0.8(1)
	0	1914.7	1.9(1)
2016	1078	932.1	0.5(2)
	991	1024.4	0.5(1)
	925	1090.8	0.5(1)
	664	1351.1	0.7(1)
	0	2016.2	4.6(2)
2127	991	1135.1	0.4(2)
	925	1200.8	0.3(1)
	664	1462.2	6(2)
	545	1581.8	0.4(1)
	0	2127.1	0.9(1)
		1175.3	2.8(1)
		1760.4	2.6(1)

placement of high-energy γ decays with no observable coincidences from new excited levels. Coincidence sums pertaining to these levels added confidence to their placement in the level scheme. When possible, decay half-lives were checked to be certain that these transitions arose from ^{109}Sb β decay.

The proposed level scheme for this experiment is in excellent agreement with ^{106}Cd$(\alpha,n\gamma)^{109}$Sn results presented in Ref. [7]. However, the level at 664 keV was not included in the $(\alpha,n\gamma)$ study, contrary to the observations in this and other ^{109}Sn studies [4,6]. In Fig. 5 coincidences with the 247- and 261-keV γ rays are shown. Both of these transitions depopulate the level at 925-keV, feeding the 678- and 664-keV levels, respectively. The presence of two 14-keV doublets (0–14 keV and 664–678 keV) is confirmed. The intensity ratio of the 678/664 transitions in the 247-keV coincidence spectrum was used to apportion the intensity of the 664-keV doublet.

Two transitions, at 1175 and 1760 keV, were observed with significant intensity and correct decay half-lives but could not be placed in the energy level scheme. Due to the lack of coincidence with any other known transitions, these transitions may arise from previously unobserved levels.

A detailed analysis of the electromagnetic transition intensities entering and exiting each known state was performed. The intensity difference may be attributed to the β feeding in the Sb decay. For example, the transition intensity deexciting the $3/2^+$ level at 925 keV should be significantly higher than the γ intensity feeding this state due to β feeding from parent decays. A state not fed in the β decay should have equal intensities entering and exiting.

Intensity differences were calculated for all known states but the ground and first excited states. The fraction of total β feeding was then determined from the intensity differences. The β population of the $5/2^+$ ground state and $7/2^+$ first excited state cannot be directly measured using our experimental setup. Therefore, the fraction of β feeding to these states was estimated using values extrapolated from ^{111}Sb $\rightarrow ^{111}$Sn β decay where the $5/2^+$ level is an excited state whose intensity can be measured directly. The extrapolated values assumed identical $\log ft$ values. The $\log ft$ for the $\pi(5/2^+)$ to $\nu(5/2_1^+)$ β decay of ^{111}Sb is 5.41, while the $\pi(5/2^+)$ to $\nu(7/2_1^+)$ is 6.1 using the recommended Q-value of 5.1 MeV [9]. The $\log ft$ for the favored $\pi d_{5/2}$ to $\nu(3/2_1^+)$ Gamow-Teller decay is 4.87.

For ^{109}Sn, two separate extrapolations were performed. The first extrapolation assumed that the $\pi(5/2^+)$ to $\nu(5/2_1^+)$ transition was identical to ^{111}Sn. For a $\log ft$ of 5.41, a 20% β branching to the ground state is calculated. The fraction of branching to the $7/2_1^+$ state was determined assuming a $\log ft$ value equal to 6.1. The remaining 76% β feeding was distributed relative to the γ intensity differences calculated for each excited state. Results are shown in Table II with associated $\log ft$ values.

The second extrapolation assumed that the $\pi(5/2^+)$ to $\nu(3/2_1^+)$ transition was identical to that of ^{111}Sn. The β branching to the $7/2_1^+$ state was determined from a ratio. The intensity to the $7/2^+$ state was one-fifth of the intensity to the $5/2_1^+$ state in the first extrapolation. This is similar to ^{111}Sn,

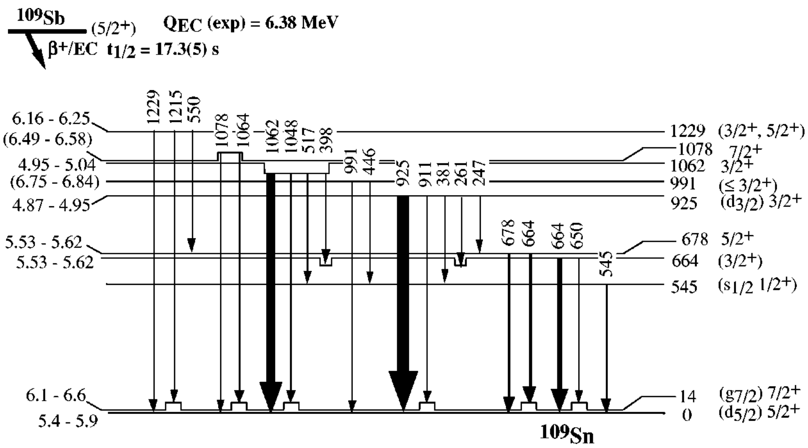

FIG. 3. Proposed level scheme ($E < 1250$ keV) for ^{109}Sn following ^{109}Sb β decay. Transition energies and levels are in keV; γ intensities relative to the $d_{3/2}$-$d_{5/2}$ transition are schematically displayed by arrow thickness. A range of proposed log *ft* values are also shown for the extrapolations presented in Table II. The decay Q value has been experimentally determined [23].

where the feeding ratio is $\sim 1{:}4$. The total intensity of the $5/2_1^+$ and $7/2_1^+$ states in the second extrapolation was determined to be 7.2%; the intensity was split in a 1:5 ratio of 1.2% and 6.0% for the $7/2^+$ and $5/2^+$ states, respectively. These results are shown in Table II with associated log *ft* values.

The second approach removes intensity from the ground state and spreads it to higher energy states. With the exception of the ground and first excited state, the log *ft* values for the two extrapolations differ by less than 0.1 units. Furthermore, both analyses suggest three highly β-fed states at 925, 1062, and 1496 keV.

B. ^{107}Sn

The β-decay half-life of ^{107}Sb was measured by observing the intensity of the known 151-keV and 1280-keV transitions as a function of time. These intensities are plotted in Fig. 6 relative to the time following tape movement. The half-life was determined to be 4.0(2) s by a weighted least-squares fit to the data. This compares well with the previous value of 4.6(8) s from Shibata *et al.* [5].

The use of the low-energy Ge detector significantly enhanced the resolution and intensity for the known 151-keV transition as compared to the prior data set of Ref. [6]. Transition energies and intensities for ^{107}Sn were derived from γ-singles, γ-γ coincidences, and γ-time data. As in the ^{109}Sn analysis, use of the time data allowed for accurate intensity values to be determined. The β decay of ^{107}Sb had the shortest observed half-life in this experiment, allowing time-gated γ-energy spectra to be used to show only those transitions that belong to ^{107}Sn. An example is shown in Fig. 7. The γ-energy spectrum collected within 5.5–9.0 s following a tape move was subtracted from the spectrum collected during the initial 3.5 s. Transitions arising from the long-lived species decayed equally during both the time segments and subtracted to zero. Transitions belonging to ^{107}Sb β decay were predominately present in the first time segment only, and appear as clear peaks in the subtracted spectrum.

From the γ-γ and time data, an energy level scheme is proposed in Fig. 8. Transitions are also shown in Table III with intensities relative to the $3/2_1^+ \rightarrow 5/2_1^+$ 1280 keV γ decay. Small peaks are observed at 1619 and 2045 keV in the

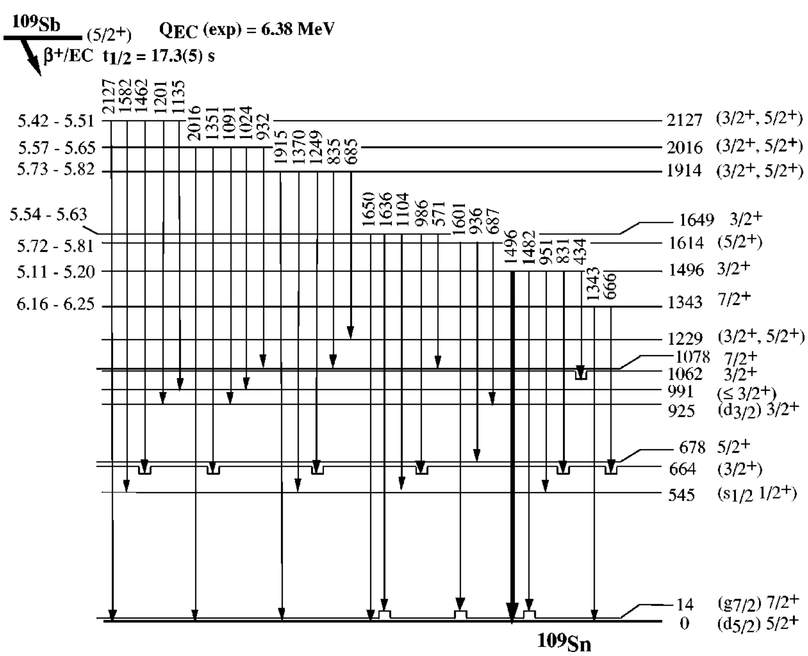

FIG. 4. Proposed level scheme ($E > 1250$ keV) for ^{109}Sn following ^{109}Sb β decay. Transition energies and levels are in keV; γ intensities relative to the $d_{3/2}$-$d_{5/2}$ transition are schematically displayed by arrow thickness. A range of proposed log *ft* values are also shown for the extrapolations presented in Table II. The decay Q value has been experimentally determined [23].

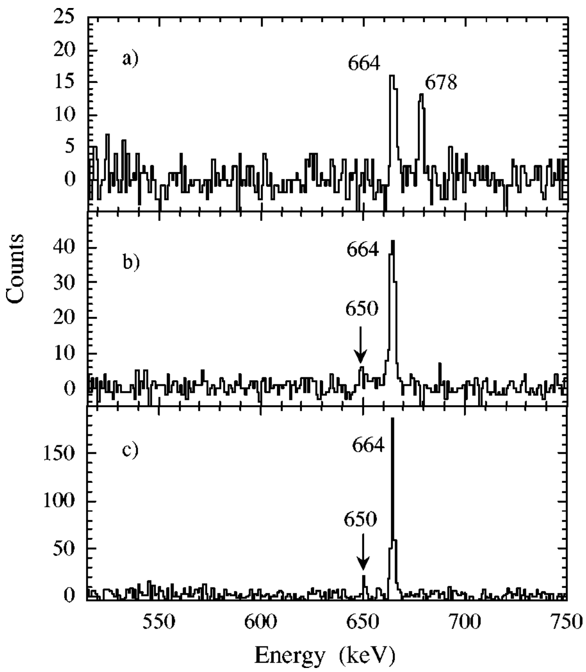

FIG. 5. Coincidence spectra for the (a) 247-keV and (b) 261-keV transitions. Both the γ's depopulate the 925-keV level to the levels at 678 and 664 keV, respectively. Observation of both 678- and 664-keV transitions in coincidence with the 247-keV γ ray suggests decays of 678→0 and 678→14 keV. Only a 664-keV transition is observed in coincidence with 261 keV, supporting a level at 664 keV with a strong decay branch to the ground. A small peak at 650 keV may also be observed, and is suggested to be a transition of 664→14 keV. In Fig. 5(c), the sum of 261-, 985-, and 1350-keV coincidence spectra is shown. These three γ rays feed the 664-keV level and show the weak 650-keV transition to the 14-keV level.

singles and time data, but do not show the correct time dependence for the ^{107}Sb decay. They have not been identified in a neighboring decay scheme. We have included them in Table III, but not in the energy level scheme.

The 704, 818, and 970 keV levels all appear to decay to the $7/2^+$ first excited state, suggesting $J^\pi \geqslant 3/2^+$. The coincidence spectrum with the 151-keV decay from the $7/2^+$ state is shown in Fig. 9. The peak at 553 keV (704 →151 keV) is questionable, but cannot easily be ignored. The weak branching intensity is similar to the 650-keV decay between the $5/2^+_2$ and $7/2^+_1$ states in ^{109}Sn. A strong peak at 667 keV (818→151 keV) and a weak peak at 819 keV (970→151 keV) are more easily identified. Due to the high intensity of the 667-keV decay from the 818-keV level, a $5/2^+$ spin and parity is proposed for this level. The low intensity of decays from the 704 and 970 keV levels suggests $3/2^+$ assignments, although $5/2^+$ or $7/2^+$ spins are also possible. The 819-keV peak may arise from the 818 →0(818 keV) transition in coincidence with a 970 →818(152 keV) decay. The inset of Fig. 9 shows the low-energy portion of the coincidence spectra. A peak at 152 keV is not observed, supporting a 970→151(819 keV) assignment.

Intensity differences for γ feeding and decays were calculated for all states but the ground state. From these differences, the fraction of total β feeding was determined. For the ground state, the level of β feeding was extrapolated from ^{111}Sn by assuming identical log ft values for ^{111}Sb→^{111}Sn decay. Two extrapolations were performed similar to what was done for ^{109}Sn. Either the $\pi(5/2^+)$ to $\nu(5/2^+_1)$ or the $\pi(5/2^+)$ to $\nu(3/2^+_1)$ transition was assumed to be identical to ^{111}Sn. Results are shown in Table IV. Both the 704- and 970-keV states appear to be fed in the β decay, suggesting spins greater than 1/2. However, due to the large decay Q value and low production cross section, either of these levels may be populated indirectly by many weak γ rays from higher energy levels not observed in this experiment. As such, the β feeding and the associated log ft values should be viewed as lower limits.

IV. DISCUSSION

A number of low-spin states have been identified in ^{109}Sn and ^{107}Sn. These states may be attributed to single-particle and cluster configurations.

A. Single-particle states

Prior to this work, the lightest odd-mass Sn isotope for which well-established data existed for all the five single-particle states ($\nu d_{5/2}$, $\nu g_{7/2}$, $\nu s_{1/2}$, $\nu d_{3/2}$, $\nu h_{11/2}$) was ^{111}Sn. The structure of ^{111}Sn is well known due to the availability of both (p,d) and polarized (d,t) data from stable ^{112}Sn in addition to in-beam and decay data. These states are not true single-particle states as there is some mixing with other configurations. However, the single-particle label is used for the states comprised of the largest component of single-particle character. The $5/2^+_1$ and $7/2^+_1$ states of the light Sn isotopes are estimated to have approximately 80% single particle character, while the $3/2^+_1$ and $1/2^+_1$ states are more heavily mixed.

The ground state of ^{111}Sn is $7/2^+$, arising from the $\nu g_{7/2}$ orbital. The $\nu d_{5/2}$ orbital lies at the low excitation energy of 154 keV. These levels are strongly populated in the neutron pickup reaction with $l=2$ and 4, respectively. As the Fermi surface moves down from the subshell closure at $N=64$, the order of the $\nu g_{7/2}$ and $\nu d_{5/2}$ states is expected to change near $A=109$. Therefore, the $\nu g_{7/2}$ and $\nu d_{5/2}$ orbitals are predicted to lie very near each other in ^{109}Sn. In the initial in-beam and decay experiments, a pair of nearly degenerate orbitals of low energy were not observed. The ground state was assumed to be $J=7/2$ due to atomic-beam magnetic resonance results [10], and this spin was used in much of the early work. More recently, a hyperfine splitting experiment suggested a $J=5/2$ ground state spin [11]. This spin assignment agrees with β-decay studies of ^{109}Sn→^{109}In [12], and was confirmed in a high-spin γ-decay study that found evidence for a very low-lying $7/2^+$ state at 13 keV above the $5/2^+$ ground state [13]. The presence of this $7/2^+$ state requires a restructuring of the levels in ^{109}Sn that has not been reflected completely in the literature.

TABLE II. β decay feeding intensities in ^{109}Sn. The difference between γ feeding and decay intensities was attributed to β population. Intensity differences relative to the 925-keV transition and fraction of the total are shown. Values for the ground and first excited state are extrapolated with suggested errors. Calculated log ft values for each state are also shown, in which the experimental $Q_{EC}=6.38$ MeV [23] was used. In the last column proposed spins and parities for each level are shown.

Level energy (keV)	γ Intensity difference	β Feeding[a] (%)	log ft [a]	β Feeding[b] (%)	log ft[b]	J^π ($\hbar$)
0		20	5.41	6	5.9	$5/2^+$
14		4	6.1	1.2	6.6	$7/2^+$
545	0(1)	0.0(2)		0.0(3)		$1/2^+$
664	25(3)	6.8(6)	5.62	8.3(7)	5.53	$(3/2^+)$
678	36(2)	6.7(5)	5.62	8.2(7)	5.53	$5/2^+$
925	11.5(7)	24.8(3)	4.95	30.2(4)	4.87	$3/2^+$
991	1.4(2)	0.3(1)	(6.84)	0.37(6)	(6.75)	$(\leqslant 3/2^+)$
1062	79(1)	17.6(4)	5.04	21.5(5)	4.95	$3/2^+$
1078	2.3(4)	0.50(8)	(6.58)	0.6(1)	(6.49)	$7/2^+$
1229	9.5(2)	2.1(1)	5.89	2.57(5)	5.80	$(3/2^+,5/2^+)$
1343	3.7(2)	0.81(5)	6.25	0.99(6)	6.16	$7/2^+$
1496	35.1(7)	7.8(2)	5.20	9.5(2)	5.11	$3/2^+$
1614	7.5(3)	1.65(7)	5.81	2.02(8)	5.72	$(5/2^+)$
1649	10.8(4)	2.40(8)	5.63	2.9(1)	5.54	$3/2^+$
1914	5.2(6)	1.2(1)	5.82	1.4(2)	5.73	$(3/2^+,5/2^+)$
2016	6.7(3)	1.49(8)	5.65	1.8(1)	5.57	$(3/2^+,5/2^+)$
2127	8(2)	1.8(3)	5.51	2.2(4)	5.42	$(3/2^+,5/2^+)$

[a]The first extrapolation assumed a log $ft=5.41$ for the $\nu d_{5/2}$ level.
[b]The second assumed log $ft=4.87$ for the $\nu d_{3/2}$ level.

For ^{107}Sn, the ground state is assumed to be $5/2^+$ from systematics and β-decay experiments. The $\nu g_{7/2}$ state is assumed to lie at 151 keV, as an $M1$ transition from this level has been observed with significant intensity.

The single-particle $\nu s_{1/2}$ state comprises the ground state for the odd-ASn isotopes with $113 \leqslant A \leqslant 119$, and is known to lie at 255 keV in ^{111}Sn from the transfer reaction experiments [14]. For the lighter odd-A Sn isotopes, the excitation energies of the single quasiparticle ($g_{7/2}$, $s_{1/2}$, $d_{3/2}$, and $h_{11/2}$) are expected to increase with respect to the $\nu d_{5/2}$ ground state toward the single-particle configurations in ^{101}Sn. The $h_{11/2}$ and $g_{7/2}$ quasiparticle states can be observed in heavy-ion fusion experiments directly following a reaction. The $d_{3/2}$ quasiparticle state is heavily populated in the allowed Gamow-Teller spin-flip β decay from the odd-$\pi d_{5/2}$ Sb parents. In contrast, the $s_{1/2}$ quasiparticle state is not populated directly in heavy-ion reactions, nor is it directly fed in the β decay. The position of the $s_{1/2}$ single-quasiparticle level must therefore be indirectly inferred from the lack of β feeding and γ decays to the low-energy $g_{7/2}$ level.

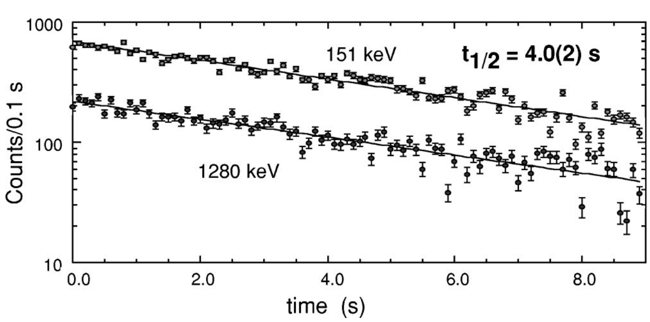

FIG. 6. Half-life determination for ^{107}Sb. Intensities of the 151- and 1280-keV transitions are shown as a function of time following a tape movement. A weighted least-squares fit to these data suggests a 4.0(2) s for the β^+/EC-decay half-life of ^{107}Sb.

In ^{109}Sn, neither the 545-keV nor the 991-keV states appear to be fed in the β decay. Nor do these states have decays to the $7/2^+$ first excited state, supporting a possible $1/2^+$ spin. From comparisons to the heavier odd-A Sn isotopes, the 545-keV level emerges as the best candidate for the $\nu s_{1/2}$ single-quasiparticle state identified in this study.

Angular distribution measurements by Dankó *et al.* using the ^{106}Cd$(\alpha,n\gamma)^{109}$Sn reaction suggested a $J^\pi=3/2^+$ spin and parity for the 545-keV level [7]. The ^{106}Cd target used was 77.3% pure; if a reasonable fraction of the remaining 32.7% was comprised of ^{112}Cd(24.1%nat.), the 545-keV γ ray might have been contaminated by the 544.7-keV doublet of ^{112}Cd$(\alpha,p\gamma)^{115}$In. The 545-keV γ rays deexcite levels at 1486.1 ($9/2^+$) and 1478.5 keV in ^{115}In [15].

Possible evidence for contamination in the Cd+α study may be seen by the large intensity observed for the 545-keV γ ray. The $J^\pi=3/2^+$ states at 925, 1062, and 1496 keV were observed only weakly. Furthermore, only the 1104- and 446-keV transitions were observed in coincidence with the 545-keV decay. The relatively intense 517-keV and 951-keV coincidences observed here and in Ref. [4] were not observed.

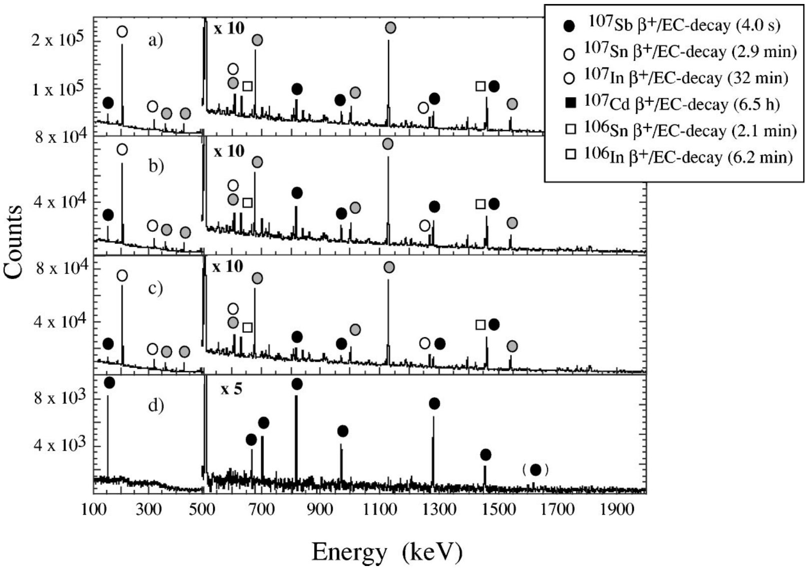

FIG. 7. Singles and time-gated γ-energy spectra for $A=107$. Figure 7(a) shows the singles spectrum for all $A=107$ recoils independent of time. Figure 7(b) displays all transitions detected within approximately 3.5 s following a tape move. Figure 7(c) shows transitions detected later than 5.5 s following a tape move. Figure 7 shows the subtraction of the late time spectrum from the earlier time. Long-lived components subtract to zero, while short-lived transitions appear as peaks. Possible peaks may be observed at 1619 keV [and 2045 keV, (not shown)], but does not exhibit the correct half-life. The peak or incorrect half-life may be due to contamination.

These missed coincidences suggest that some portion of the 545-keV intensity observed by Dankó *et al.* did not arise from ^{109}Sn, and may be the cause for the finite angular distribution coefficents.

A clear candidate for the $s_{1/2}$ level in ^{107}Sn was not identified. For the 704-keV level to have $1/2^+$ spin and parity, the 553-keV peak in the 151-keV coincidence spectrum must arise from random events. The lack of a 553-keV transition in the time subtracted data supports a random observation, but the statistics may be too poor for confirmation. Furthermore, the low-energy $1/2^+$ state cannot be directly populated in the β decay of the $5/2^+$ ^{107}Sb parent. We did not observe any γ rays in coincidence with the 704-keV transition, nor did we identify any γ rays in the singles data that may represent decays to the 704-keV level from higher-lying $3/2^+$ states. In ^{109}Sn, these decays were relatively strong and easily identified. Therefore, a $3/2^+$ spin is assigned to the 704-keV level in ^{107}Sn.

The observation of the low-lying $s_{1/2}$ state in ^{109}Sn suggests that this state may also lie at an energy lower than expected in ^{101}Sn. While the energy of this level has a little influence on the calculated shell model energies, it may play a role in the transition rates. This was observed in recent calculations for an isomeric $6^+ \rightarrow 4^+$ decay in ^{102}Sn [16]; cancellations in the matrix elements caused the calculated $B(E2)$ intensities to be sensitive to the single-particle energies of the $s_{1/2}$ and $d_{3/2}$ orbitals.

Three strongly β-fed states were observed in ^{109}Sn and ^{107}Sn: states at 925, 1062, and 1496 keV in ^{109}Sn and 970, 1280, and 1454 keV in ^{107}Sn. These states are suggested to have relatively large $d_{3/2}$ neutron quasiparticle admixtures and were assigned $3/2^+$ spins and parities. Other low-spin states were also observed in both isotopes. Tentative spins and parities have been assigned in accordance with observed β branching and γ intensities. Results are summarized in Figs. 4, 3, and 8.

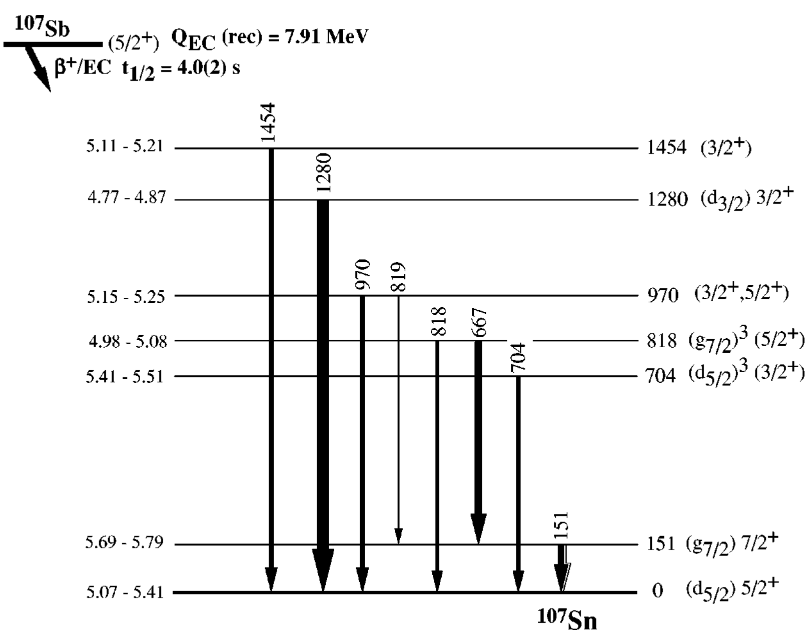

FIG. 8. Proposed level scheme for ^{107}Sn following ^{107}Sb β decay. Transition energies and levels are in keV; γ intensities relative to the $d_{3/2}$-$d_{5/2}$ transition are schematically displayed by arrow thickness. Internal conversion contributions to the intensity are denoted in white. A range of proposed $\log ft$ values are also shown for the extrapolations presented in Table II. The decay Q-value has been recommended [23].

TABLE III. γ intensities in ^{107}Sn following ^{107}Sb β decay. Energy errors are ± 0.3 keV. Intensities are relative to the 1280-keV transition.

Level energy (keV)	To level (keV)	γ-ray energy (keV)	Relative intensity
0			
151	0	151.5	64(3)
704	151	552.7	3(1)
	0	703.5	34(2)
818	151	666.6	63(3)
	0	818.2	34(2)
970	151	819.4	9(2)
	0	970.2	44(2)
1280	0	1280.1	100
1454	0	1453.9	40(3)
(1619)	0	1619.5	10(1)
(2045)	0	2045.5	7(1)

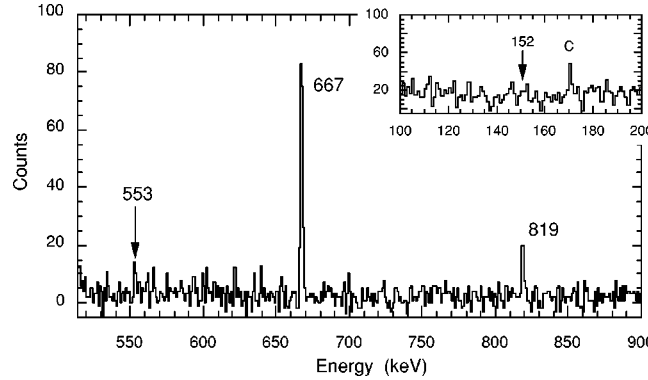

FIG. 9. Coincidences with the 151-keV transition of ^{107}Sn. A peak at 819 keV is easily observed, suggesting a transition between the 970- and 151-keV levels. A coincident transition of 152 keV is not observed, supporting the absence of a second 152-keV transition from the 970-keV to the 818-keV level. A small peak may or may not exist at 553 keV. If real, this transition would arise from the 704-keV level. The small peak at 169 keV is due to Compton scattering of the strongly produced 321-keV transition in ^{107}Cd following ^{107}In decay.

B. Cluster states

Nuclei having three particles or holes outside single closed shells may have a cluster state, in which the three particles (or holes) interact without pairing. For an odd-A nuclide with three nucleons (or holes) occupying a state $j \geqslant 5/2$, the last odd particle is responsible for the observed nuclear spin. In addition, a low-energy cluster state of $j^3 = J-1$ may be observed above the single-particle ($J=j$) state, but well below the core-coupled states. Other cluster states of $j^3 = J-2, J+2, J+1, \ldots$ lie at higher excitation energy. Secondary $3/2^+$ and $5/2^+$ states have been observed in both ^{109}Sn and ^{107}Sn below 1 MeV. These states may arise from three-quasiparticle coupling involving particles (or holes) in the $\nu d_{5/2}$ and $\nu g_{7/2}$ orbitals, respectively.

Shown in Fig. 10 are the odd-A $N=82$ isobars with $Z=51-65$. For both ^{135}I and ^{137}Cs, two $5/2^+$ levels are observed contrary to the single level in the remaining isotones. The single $5/2^+$ level is attributed to the $d_{5/2}$ proton single-particle level. The additional $5/2^+$ level in ^{135}I and ^{137}Cs is the result of the $g_{7/2}$ cluster. Three valence protons or holes in the $g_{7/2}$ orbital couple to $5/2^+$ in ^{135}I and ^{137}Cs, respectively. Such cluster structures are not observed in the other nuclides as the $g_{7/2}$ orbital contains too few or too many particles.

Spectroscopic factors from (^{3}He,d) transfer reactions [17] are shown for the $5/2^+$ levels in I and Cs. The lower $5/2^+$ state contains higher single-particle character for both isotones. However, the single-particle strength for cluster structure in ^{135}I shows a significant amount of mixing between the $d_{5/2}$ and $(g_{7/2})^3 5/2^+$ levels. Mixing between the two $5/2^+$ states in ^{135}I will push the $5/2^+_1$ level down in excitation energy, and the $5/2^+_2$ higher. This is not the case in ^{137}Cs, where the $d_{5/2}$ composition is minimal in the $5/2^+_2$ level.

Three-quasiparticle or cluster coupling was also used to describe low-lying $7/2^+$ levels on odd-mass Ag isotopes with

TABLE IV. β-decay feeding intensities in ^{107}Sn. The difference between γ feeding and decay intensities was attributed to the β population. Intensity differences relative to the 1280-keV transition and fraction of the total are shown. The fraction of β feeding for the ground state is extrapolated with an approximate error. Calculated log ft values for each state are also shown, in which the recommended $Q_{EC}=7.91$ MeV [23] was used. In the last column, proposed spins and parities for each level are shown.

Level energy (keV)	γ-Intensity difference	β feeding[a] (%)	log ft[a]	β feeding[b] (%)	log ft[b]	J^π ($\hbar$)
0		14.6	5.41	32	5.07	$5/2^+$
151	28(4)	6.9(4)	5.69	5.5(3)	5.79	$7/2^+$
704	31(2)	9.1(5)	5.41	7.2(4)	5.51	$(3/2^+)$
818	89(3)	22(1)	4.98	17(1)	5.08	$(5/2^+)$
970	54(3)	13.2(7)	5.15	10.5(6)	5.25	$(3/2^+,5/2^+)$
1280	100	25(1)	4.77	20(1)	4.87	$3/2^+$
1454	40(3)	9.8(6)	5.11	7.8(4)	5.21	$(3/2^+)$

[a]The first extrapolation assumed log ft=5.41 for the $\nu d_{5/2}$ level.
[b]The second assumed log ft=4.87 for the $\nu d_{3/2}$ level.

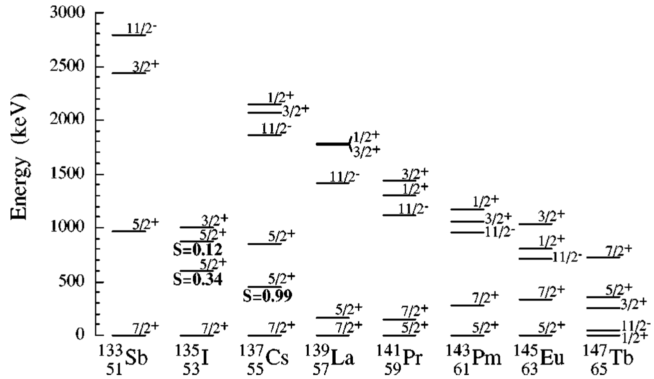

FIG. 10. Level systematics for $N=82$ isotones. The presence of the second $5/2^+$ state in ^{135}I and ^{137}Cs is attributed to $(g_{7/2})\pm 3$ cluster structures. Spectroscopic factors are adopted from Ref. [17].

three $g_{9/2}$ holes in the $Z=50$ closed shell [18]. This model was also used to explain a $3/2^+$ level at only 267 keV in ^{93}Zr, having a $(\nu d_{5/2})^3$ configuration. Similar low-energy $3/2^+$ states are not observed in either ^{91}Zr or ^{95}Zr.

Neutron clusters above the $N=50$ shell gap may also be observed in the light Sn isotopes. The close proximity of the neutron $d_{5/2}$ and $g_{7/2}$ orbitals suggests that three-quasiparticle/hole clusters may be observed for both orbitals. Experimental energy levels for the light odd-A Sn isotopes are shown in Fig. 11. For ^{115}Sn, both the $d_{5/2}$ and $g_{7/2}$ orbitals are full as the $N=64$ ^{114}Sn core is semimagic. No three-quasiparticle structures of $(d_{5/2})^3 3/2^+$ or $(g_{7/2})^3 5/2^+$ are observed or expected. The structure of ^{113}Sn, with a single hole in the $N=64$ subshell, consists of the same five quasiparticle levels below 1 MeV as compared to ^{115}Sn. The removal of two neutrons provides three holes in the $g_{7/2}$ orbital, which couple to form the second $5/2^+$ state at 755 keV in ^{111}Sn. Transfer reaction studies determine a spectroscopic factor of only $\sim 2\%$ [19,20] of the value observed for the $d_{5/2}$ ground state.

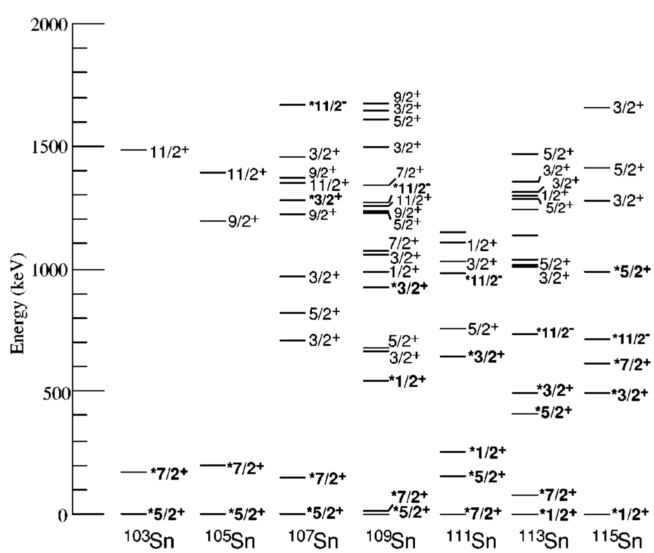

FIG. 11. Experimental energy levels for the light odd-A Sn isotopes. Single-quasiparticle neutron levels are shown in bold and with an asterisk (*).

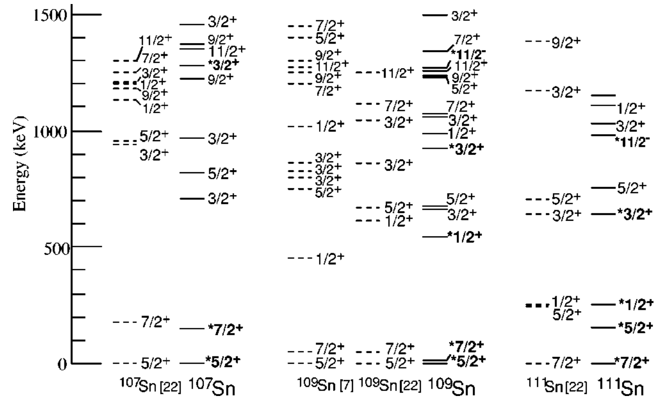

FIG. 12. Experimental (solid) and theoretical (dashed) energy levels for the light odd-A Sn isotopes. Single-quasiparticle neutron levels are shown in bold and with an asterisk (*). Calculated levels are adopted from Refs. [21] and [7].

In ^{109}Sn, three-quasiparticle/hole cluster structures may be observed for both the $g_{7/2}$ and $d_{5/2}$ orbitals. In our data, the level at 678 keV is suggested to be primarily comprised of a $(\nu g_{7/2})^{-3} 5/2^+$ configuration. In Fig. 12, experimental and theoretical energy levels for the light odd-A Sn isotopes are shown. Calculations in Refs. [21] and [7] support a $5/2^+$ level in this energy region. The calculated energy levels of Ref. [21] show only two low-energy $3/2^+$ states—presumably the $d_{3/2}$ single-quasiparticle level and a particle-core state. Calculations in Ref. [7] show three low-energy $3/2^+$ states consistent with the three states suggested from the experimental data. The level at 664 keV is proposed as the $(\nu d_{5/2})^{\pm 3} 3/2^+$ state, while the level at 925 keV is largely comprised of the $d_{3/2}$ single-neutron configuration. The third $3/2^+$ state at 1062 keV may arise from a $d_{5/2}$ or $g_{7/2}$ neutron coupled to the 2^+ core.

In ^{107}Sn, the level at 818 keV is expected to be the three-quasiparticle cluster $(\nu g_{7/2})^{-3} 5/2^+$ state, as the separation energy from the $g_{7/2}$ level is 667 keV, similar to the 664 keV observed in ^{109}Sn. The $3/2^+$ spin and parity proposed for the 704-keV level may be the $(\nu d_{5/2})^{\pm 3} 3/2^+$ state, as it is only 26 keV higher in excitation energy than a similar state at 678 keV in ^{109}Sn. The $5/2^+$ level at 819 keV and $3/2^+$ state at 970 keV closely approximate the $5/2^+$ and $3/2^+$ levels near 950 keV calculated in Ref. [21]. The strong β decay branching to the 1280-keV level suggests dominant $d_{3/2}$ single-quasiparticle configuration. Calculations in Ref. [21] do not reproduce the $d_{5/2}$ cluster state, similar to ^{109}Sn results.

V. EXTRAPOLATED SINGLE-PARTICLE LEVELS IN ^{101}Sn

Values for the single-particle energies of ^{101}Sn are presented in numerous theoretical papers available in the literature. A sample is shown in Table V. The largest divergence between the models is the placement of the $s_{1/2}$ and $g_{7/2}$ levels.

The calculated energy levels of ^{109}Sn shown in Fig. 12 by Dankó *et al.* [7] used the model of Sandulescu *et al.* The single-particle energies are shown in Table V for Ref. [21]. As seen in Fig. 12, calculations in Ref. [21] place the $1/2^+$ level of ^{109}Sn too high in energy, while Ref. [7] is too low.

TABLE V. Single-neutron energy levels (in MeV) for ^{101}Sn.

	Sandulescu [22]	Engeland [21]	Duflo [24]	Leander Wood-Saxon	Leander folded Yukawa	Leander Skyrme III [25]	Borzov [26]
$d_{5/2}$	0	0	0	0	0	0	0
$g_{7/2}$	0.5	0.20	0.5	1.45	1.09	0.47	1.899
$s_{1/2}$	1.6	2.45	0.8	2.16	2.46	2.54	2.106
$d_{3/2}$	2.2	2.54	1.6	2.86	3.22	2.44	2.262
$h_{11/2}$	2.6	3.00	2.4	2.77	3.13	3.24	2.862

These two calculations may then suggest a reasonable limit for the $s_{1/2}$ level in ^{101}Sn, i.e., 1.6 – 2.45 MeV relative to the $d_{5/2}$ ground state. A rough extrapolation from the heavier mass odd-A Sn isotopes supports placement of the $s_{1/2}$ orbital within this range.

Values for the single-particle energies shown in Table V are typically extrapolated from experimental observations near other shell closures. The Fermi level is assumed to smoothly decrease away from the shell closure. This can be seen for the $N=82$ isotones shown in Fig. 10, where excitation energies for the $d_{5/2}$ and $h_{11/2}$ single-quasiparticle orbitals smoothly decrease as Z drops from 65 to 51.

However, such an assumption may not be justified in the regions where little experimental data is available. Systematics for the Ni isotopes near $N=40$ is shown in Fig. 13. The $g_{9/2}$ intruder orbital is high in energy near $N=28$, then lowers as the neutron number increases. However, the $g_{9/2}$ level remains at a nearly constant excitation energy for the isotopes having $N=35$–39. For these isotopes, the Fermi level becomes "trapped" between the close-lying $f_{5/2}$ and $p_{1/2}$ orbitals. The additional neutrons do not significantly alter the Fermi energy, and therefore do not affect the excitation energy of the $g_{9/2}$ state.

Uncertainties in the light Sn structures may also lead to large errors for extrapolations toward ^{101}Sn. In ^{103}Sn, the $g_{7/2}$ level is suggested to be positioned at only 168 keV above the $d_{5/2}$ ground state [2]. This finding was recently confirmed in an α fine structure experiment [3]. As the excitation energy of the $g_{7/2}$ level smoothly increases from ^{111}Sn down to ^{105}Sn, the lowered energy in ^{103}Sn is unexpected. This rollover raises questions about the position for the $\nu g_{7/2}$ level in ^{101}Sn. Does the downtrend continue, suggesting a 100-keV $d_{5/2}$-$g_{7/2}$ separation energy? Or is the relatively low $\nu g_{7/2}$ level in ^{103}Sn due to an effect present in $^{105-109}$Sn, but not in ^{103}Sn or ^{101}Sn?

If the new data for ^{103}Sn is used to support a 100-keV $d_{5/2}$-$g_{7/2}$ separation energy for ^{101}Sn, this may suggest that the Fermi level may be "trapped" between the close-lying $d_{5/2}$ and $g_{7/2}$ orbitals for $N=51$–55. The $d_{3/2}$, $s_{1/2}$, and $h_{11/2}$ orbitals would then increase slightly as $N=50$ is approached, and would lie at much lower energies than that suggested in Table V.

The centroids for the Gamow-Teller spin-flip transition

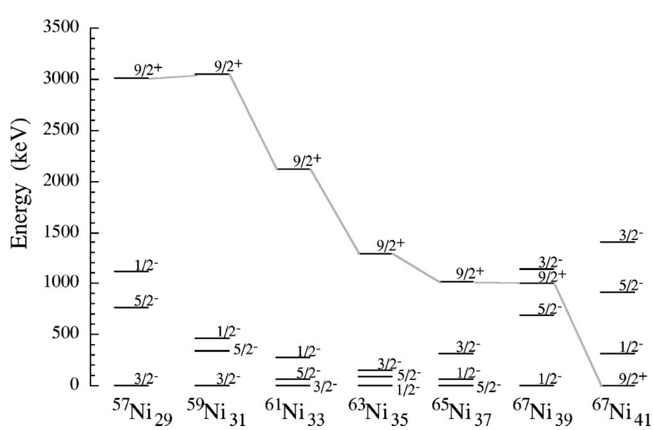

FIG. 13. Level systematics for the Ni isotopes. The nearly constant excitation energy for the $9/2^+$ state in $^{63-67}$Ni may arise from Fermi level "trapping" between the $f_{5/2}$ and $p_{1/2}$ orbitals.

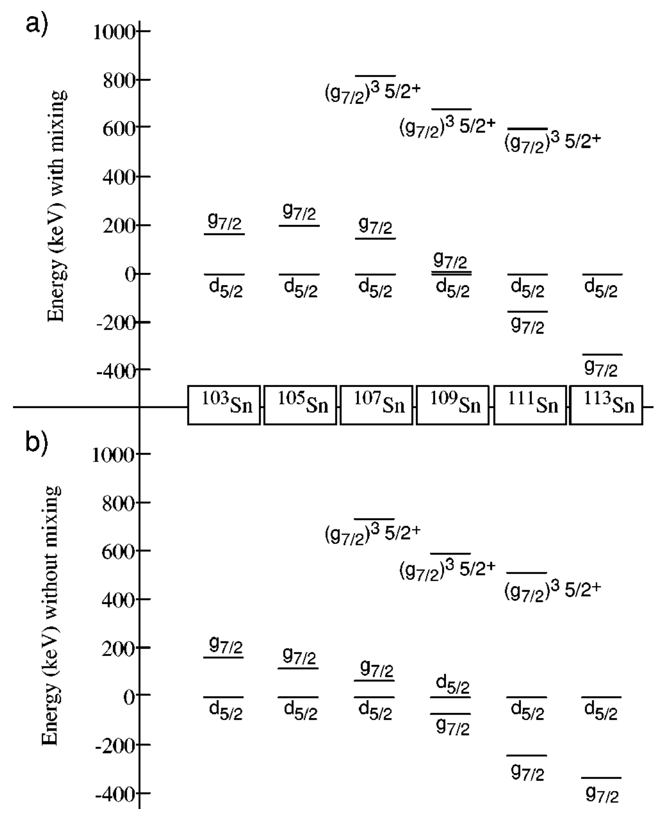

FIG. 14. Mixed and unmixed $5/2^+$ levels in $^{103-113}$Sn isotopes. Energies are shown relative to the $d_{5/2}$ state. The presence of the $(g_{7/2})^{-3}5/2^+$ cluster state in $^{107-111}$Sn may lower the $d_{5/2}$ quasiparticle state $\sim$80 keV. A potential cluster state in ^{105}Sn is assumed to lie at a similar energy as $^{107-111}$Sn.

strength using the four lowest $3/2^+$ levels in ^{109}Sn and ^{107}Sn are 1075 and 1200 keV, respectively. This would suggest that the $d_{3/2}$ level in ^{101}Sn would lie at 1750 keV by a simple linear extrapolation. While this energy is well below the predictions in Table V, it is consistent with the known $d_{5/2}$-$d_{3/2}$ spin-orbit splitting of 1656 keV for the single neutron hole levels in ^{131}Sn. This would suggest that the $s_{1/2}$ level would also lie between 1.5 and 2 MeV in ^{101}Sn. The largest difference would be for the $h_{11/2}$ orbital, which may lie below the expected range between 2.0 and 2.4 MeV. In ^{131}Sn, the $d_{5/2}$-$h_{11/2}$ separation energy is only 1415 keV.

An alternative explanation may suggest that the observed trend for the $5/2^+$-$7/2^+$ energy separation in $^{105-109}$Sn is affected by mixing between the $d_{5/2}$ single-quasiparticle state and the $(\nu g_{7/2})^3 5/2^+$ cluster state. Mixing between these two states would lead to an exaggerated lowering of the $5/2^+$ ground state relative to the first excited $g_{7/2}$ state in the isotopes where cluster states are present. The observed structures could arise from a small ($\sim$100–150 keV) depression for the ground state if matched by a similar increase in the cluster excitation energy. This is shown in Fig. 14. The effect of mixing will be weak in ^{103}Sn due to the relatively large $d_{5/2}$-$g_{7/2}$ separation energy. Moving three neutrons into the $g_{7/2}$ orbital will require a significant amount of energy; the $5/2^+$ cluster state will thus lie high in excitation energy and mix little with $5/2^+$ ground state. As more neutrons are added, the $\nu g_{7/2}$ nears the Fermi surface and the effects of mixing are significant. For ^{113}Sb, with a single neutron hole in the $N=64$ subshell, the cluster state is no longer available. Mixing effects are maximized for $N=55$, 57, and 59 neutrons, respectively, as three particles/holes are readily available for both the $d_{5/2}$ and $g_{7/2}$ orbitals.

Similar to ^{113}Sb, the cluster state is unavailable in single-neutron ^{101}Sn. Systematics for the $d_{5/2}$ and $g_{7/2}$ orbitals in the lighter $N=51$ isotones has recently been extended to ^{99}Cd, where the separation energy is 441 keV [27]. A $d_{5/2}$-$g_{7/2}$ separation energy within 100–300 keV is proposed for ^{101}Sn by comparison to the systematics and unmixed levels of Fig. 14. A separation larger than 441 keV would be unexpected.

VI. CONCLUSIONS

Low-energy, low-spin levels were observed and characterized in ^{109,107}Sn following ^{109,107}Sb β decay. Combined with the recent data (i.e., Ref. [7]), the structure of ^{109}Sn is now well established below 1.5 MeV.

The gradual rise in the β-decay strength centroid for the low-energy $3/2^+$ levels, combined with the low $5/2^+$-$7/2^+$ separation energy in ^{103}Sn can be used to support Fermi level ''trapping'' between close-lying $d_{5/2}$ and $g_{7/2}$ single-quasiparticle neutron levels. The Fermi level rises only slightly as N decreases below 57. Consequently, extrapolations for the energies of the $s_{1/2}$, $d_{3/2}$, and $h_{11/2}$ shown in Table V lead to energies that may be too high by 500 to 1000 keV.

Moreover, new data for ^{107}Sn and a more complete level scheme for ^{109}Sn may demonstrate trends for cluster structures in the light Sn isotopes, which may offer another possible approach for understanding the low $d_{5/2}$-$g_{7/2}$ separation energy in ^{103}Sn. These data support an intermediate position near 2.0 MeV for the $s_{1/2}$ neutron quasiparticle level in ^{101}Sn, as compared to values shown in Table V. For the $\nu g_{7/2}$ position, a quantitative evaluation of mixing between the $5/2^+$ cluster state with the $\nu d_{5/2}$ ground state is necessary to improve the precision of an estimated position of 250(150) keV.

ACKNOWLEDGMENT

Support for this work was provided by the U.S. Department of Energy under Contract Nos. DE-FG02-91ER-40609, DE-FG02-88ER40417, DE-FG02-94ER-40834, and W-31-109-ENG-38.

[1] W.B. Walters, in Nuclear Fission and Fission-Product Spectroscopy, edited by Gabriele Fioni, Herbert Faust, Stephan Oberstedt, and Franz-Josef Hamlasch, AIP Conf. Proc. No. 447 (AIP, Woodbury, NY, 1998), p. 196.
[2] C. Fahlander *et al.*, Phys. Rev. C **63**, 021307(R) (2001).
[3] D. Seweryniak, W. B. Walters, A. Wöhr, P. Battacharya, A. Heinz, J. J. Ressler, and J. Shergur, Proceedings of the Conference on Exotic Nuclei and Atomic Masses 2001, Hämeenlinna, Finland, 2001.
[4] M.G. Johnston, I.S. Grant, P. Misaelides, P.J. Nolan, P. Reuser, R. Kirchner, O. Klepper, E. Roeckl, and P. Tidemand-Peterson, J. Phys. G **8**, 1405 (1982).
[5] M. Shibata *et al.*, Phys. Rev. C **55**, 1715 (1997).
[6] J. J. Ressler, D. Seweryniak, L. Conticchio, W. B. Walters, J. Wauters, C. Bingham, R. de Haan, B. Foy, and C. N. Davids, in *Proceedings of the Conference on Exotic Nuclei and Atomic Masses, Bellaire, MI*, edited by B. Sherrill, D. Morissey, and C. N. Davids (AIP, New York, 1998), p. 455.
[7] I. Dankó *et al.*, Nucl. Phys. **A646**, 3 (1999).
[8] D.C. Radford, Nucl. Instrum. Methods Phys. Res. A **361**, 297 (1995).
[9] J. Blachot, Nucl. Data Sheets **77**, 299 (1996).
[10] W. Hogervorst, C. Ekstrom, S. Ingelman, and G. Wahnberg, Phys. Scr. **9**, 317 (1974).
[11] J. Eberz *et al.*, Nucl. Phys. **A464**, 9 (1987).
[12] V.P. Burminsky and O.D. Kovrigin, Izv. Akad. Nauk SSSR, Ser. Fiz. **45**, 123 (1981).
[13] L. Kaubler *et al.*, Z. Phys. A **351**, 123 (1995).
[14] D.G. Fleming, Can. J. Phys. **60**, 428 (1982).
[15] J. Blachot, Nucl. Data Sheets **86**, 151 (1999).
[16] M. Lipogavšek *et al.*, Phys. Lett. B **440**, 246 (1998).
[17] B.H. Wildenthal, E. Newman, and R.L. Auble, Phys. Rev. C **3**, 1199 (1971).
[18] V. Paar, Nucl. Phys. **A211**, 29 (1973).
[19] S. Gales, E. Gerlic, G. Duhamed, G. Perrin, C. Perrin, and V. Comparat, Nucl. Phys. **A381**, 40 (1982).
[20] P.J. Blankert, H.P. Blok, and J. Blok, Nucl. Phys. **A356**, 74 (1981).

[21] T. Engeland, M. Hjorth-Jensen, A. Holt, and E. Osnes, Phys. Scr. **T56**, 58 (1995).
[22] N. Sandulescu, J. Blomqvist, and J.J. Liotta, Nucl. Phys. **A582**, 257 (1995).
[23] G. Audi and A.H. Wapstra, Nucl. Phys. **A595**, 409 (1995).
[24] J. Duflo and A.P. Zucker, Phys. Rev. C **59**, R2347 (1999).
[25] G.A. Leander, J. Dudek, W. Nazarewicz, J.R. Nix, and Ph. Quentin, Phys. Rev. C **30**, 416 (1984).
[26] I.N. Borzov, S.A. Fayans, E. Krömer, and D. Zwaischa, Z. Phys. A **355**, 117 (1996).
[27] M. Lipoglavsek, C. Baktash, M.P. Carpenter, D.J. Dean, C. Fahlander, M. Hjorth-Jensen, R.V.F. Janssens, A. Likar, J. Nyberg, S.D. Paul, A. Piechaczek, D.C. Radford, D. Rudolph, D. Seweryniak, D.G. Sarantites, M. Vencelj, and C.H. Yu, Nucl. Phys. **A682**, 399c (2001).